HHS Public Access

Author manuscript

Matrix Biol. Author manuscript; available in PMC 2020 May 01.

Published in final edited form as:

Matrix Biol. 2019 May ; 78-79: 165–179. doi:10.1016/j.matbio.2018.05.002.

Prostate tumor cell exosomes containing hyaluronidase Hyal1 stimulate prostate stromal cell motility by engagement of FAK-mediated integrin signaling

Caitlin O. McAtee[1,*], **Christine Booth**[1,*], **Christian Elowsky**[2], **Lei Zhao**[4], **Jeremy Payne**[1], **Teresa Fangman**[2], **Steve Caplan**[3,5], **Michael D. Henry**[4], and **Melanie A. Simpson.**[6]

[1]Department of Biochemistry, University of Nebraska, Lincoln, NE

[2]Morrison Microscopy Facility, University of Nebraska, Lincoln, NE

[3]Department of Biochemistry and Molecular Biology, University of Nebraska Medical Center, Omaha, NE

[4]Department of Molecular Physiology and Biophysics; Holden Comprehensive Cancer Center, University of Iowa Carver College of Medicine; Iowa City, IA

[5]Fred and Pamela Buffett Cancer Center, Omaha, NE

[6]Department of Molecular and Structural Biochemistry, North Carolina State University, Raleigh, NC

Abstract

The hyaluronidase Hyal1 is clinically and functionally implicated in prostate cancer progression and metastasis. Elevated Hyal1 accelerates vesicular trafficking in prostate tumor cells, thereby enhancing their metastatic potential in an autocrine manner through increased motility and proliferation. In this report, we found Hyal1 protein is a component of exosomes produced by prostate tumor cell lines overexpressing Hyal1. We investigated the role of exosomally shed Hyal1 in modulating tumor cell autonomous functions and in modifying the behavior of prostate stromal cells. Catalytic activity of Hyal1 was necessary for enrichment of Hyal1 in the exosome fraction, which was associated with increased presence of LC3BII, an autophagic marker, in the exosomes. Hyal1-positive exosome contents were internalized from the culture medium by WPMY-1 prostate stromal fibroblasts. Treatment of prostate stromal cells with tumor exosomes did not affect proliferation, but robustly stimulated their migration in a manner dependent on Hyal1 catalytic activity. Increased motility of exosome-treated stromal cells was accompanied by enhanced adhesion to a type IV collagen matrix, as well as increased FAK phosphorylation and integrin engagement through dynamic membrane residence of β1 integrins. The presence of Hyal1 in tumor-derived exosomes and its ability to impact the behavior of stromal cells suggests cell-cell

Corresponding Author: Melanie A. Simpson, Ph.D. 128 Polk Hall, 120 Broughton Drive, Raleigh, NC 27695-7622; phone (919) 515-5680; msimpso3@ncsu.edu.

*These authors contributed equally.

communication via exosomes is a novel mechanism by which elevated Hyal1 promotes prostate cancer progression.

Keywords

hyaluronan; hyaluronidase; prostate cancer; cell motility; exosomes; stromal-epithelial crosstalk

INTRODUCTION

Hyaluronan (HA) homeostasis is required for normal cell and tissue function, but the altered expression of HA synthesis and turnover enzymes is clinically and functionally implicated in progression of numerous diseases, including cancer [1–7]. Elevated expression of the hyaluronidase Hyal1 accelerates metastasis of prostate cancer in mice, by increasing cell motility, rate of tumor cell vesicle trafficking, and plasma membrane receptor turnover [8–11]. Hyal1 is a key HA turnover enzyme that has unique functions among the hyaluronidases in that it both facilitates endocytic HA uptake and actively catalyzes HA degradation in acidic conditions. Low molecular weight HA (LMW-HA) polymers such as those produced by Hyal1 impact cell signaling differently than high molecular weight HA (HMW-HA) through altered affinity for cell surface receptors and also as a result of reduced multivalency, which affects binding avidity and alters local receptor clustering [12, 13]. These effects are incompletely understood and also reflect relative HA metabolic enzyme and receptor profiles, as well as transient cellular microenvironment fluctuations.

Exosomes are small, stable vesicles with an average diameter of 50–100 nm that are produced constitutively by most cell types [14, 15]. These vesicles can be detected in plasma and other body fluids, where they are significantly more abundant in cancer patients, increase with aggressiveness of the tumor, and often have diagnostic and prognostic potential [16–19]). In normal conditions, exosomes are formed from the inward budding of intracellular multivesicular bodies (MVBs) and are released to the extracellular space when the MVBs fuse with the plasma membrane [20, 21]. However, numerous reports have also defined alternative biogenesis routes that originate in endosomes, lysosomes, and other digestive organelles [15, 22, 23]. Exosomes are distinguished from larger extracellular vesicles based on size, shape, mechanism of biogenesis, and marker proteins. Sorting of exosomal cargo appears to be a regulated process, with specific biomolecules (proteins and RNA species) enriched in exosomes [24], which can then be carried from a source cell to a target cell (Reviewed in [18]). In cancer, exosomes contribute to the formation of a pre-metastatic niche by transferring molecular information through the circulation from primary tumor cells to distant tissues, which then induces physiological changes in the cells of the target tissue to promote invasion and colonization by tumor cells [25, 26]. Exosomes released from prostate tumor cells under hypoxic conditions have higher levels of tetraspanins, heat shock proteins, and multiple signaling molecules [27], which enhance motility and invasion in cells that have not been exposed to hypoxia. Thus, the microenvironment conditions within a tumor have the potential to support cancer cell survival by promoting release of specifically formulated exosomes [27].

Cancer-associated fibroblasts are unique to the stromal microenvironment of tumors. Relative to normal fibroblasts, they are characterized by increased proliferation, contractility, motility, secretion of growth factors and altered extracellular matrix production [28, 29]. Signals emitted by tumor cells, some of which are exosomally delivered, can activate fibroblasts to a cancer-associated fibroblast phenotype [30, 31]. For example, exosomes containing TGF-β1 induce prostate stromal fibroblast transformation in a manner dependent on exosomal heparan sulfate that is not replicated by soluble TGF-β1 alone [32]. Moreover, the enzyme heparanase, which degrades heparan sulfate, controls exosome secretion, contents, and promotion of endothelial cell invasion [33]. Either overexpression of heparanase or treatment with exogenous heparanase increases tumor exosome secretion rate, and this phenomenon is dependent upon its catalytic activity [33].

Prostate tumor cells secrete more exosomes than normal prostate epithelial cells, and these exosomal products are capable of altering gene expression in stromal cells [30–32, 34]. We previously found prostate tumor cells overexpressing Hyal1 had accelerated vesicular trafficking rates that increased autocrine proliferation and motility through changes in cell surface integrins and cadherins [35]. These alterations were dependent on Hyal1 catalytic activity, but the activity of Hyal1 in the extracellular space at neutral pH is negligible. Therefore, we hypothesized that Hyal1 may be present in exosomes shed by tumor cells. In this report, we used prostate tumor cells overexpressing wild-type or catalytically inactive Hyal1 to examine the impact of Hyal1 expression and activity on the rate of tumor cell exosome secretion, and the ability of the respective exosomal populations to modulate the phenotype of prostate stromal fibroblasts in culture.

RESULTS

Hyal1 is present in exosomes secreted by Hyal1-overexpressing cells

To examine the possible role of Hyal1 in exosome-mediated cellular communication, we first characterized its expression in fractionated conditioned media from our previously reported 22Rv1 transfectants selected for expression of Hyal1 with a C-terminal fusion to the pH stable reporter tdTomato (tdT [35]). In the absence of stable Hyal1 overexpression, these cells normally express negligible Hyal1 but also have low surface-associated HA due to very little HA synthase expression. Using differential centrifugation, we obtained enriched fractions containing larger extracellular vesicles (MV), exosomes (EX), and soluble proteins (CM), and compared these to whole cell lysates (WCL) by western analysis of Hyal1 expression. Hyal1 protein was abundant in the WCL (not shown), large extracellular vesicles, and secreted exosomes of cells overexpressing Hyal1WT-tdT (Fig 1A). We have shown that Hyal1 is secreted to the conditioned media as part of its normal trafficking itinerary [35], but a significant portion of Hyal1 was also secreted within or in tight association with exosomes. Moreover, the amount of Hyal1 was higher in exosomes than in larger extracellular vesicles.

Hyal1 catalytic activity is required for inclusion of Hyal1 protein in exosomes

We next tested whether exosomal secretion of Hyal1 was dependent on its enzymatic activity and if its expression impacted overall exosome production. We compared exosomal

Hyal1 and the exosomal protein CD63 in lines expressing wild-type Hyal1 (Hyal1WT-tdT), a catalytically inactive point mutant (Hyal1E131Q-tdT), or an active mutant with reduced binding affinity (Hyal1Y202F-tdT) (Fig 1A, 1B). Like the wild-type enzyme, Hyal1E131Q-tdT was detected in the microvesicle and exosomal fractions, but in contrast to wild-type protein, the Hyal1E131Q-tdT fusion protein was concentrated in the microvesicle fraction relative to the exosomal fraction. Hyal1E131Q-tdT is secreted into the conditioned media [35], but in lower amounts, so its limited presence in the soluble fraction here is expected. CD63 is a vesicular membrane tetraspanin highly concentrated in exosomes [36]. Comparable levels of CD63 and overall protein expression in the exosomal fraction of all Hyal1 transfectant lines (Fig 1B, 1C) validated the integrity of vesicle preparations and confirmed that differences in specific protein expression were not due to numbers of vesicles.

When Hyal1 fusion protein expression was normalized to CD63 signal, some variability was observed in the amounts of Hyal1-tdT protein present in the CD63-positive vesicle fraction (Fig 1D). Therefore, we compared several transfectants with a range from low to high Hyal1WT-tdT expression. When we correlated Hyal1 expression in WCL to that secreted in exosomes, there was a strong correlation between levels of expression in WCL and exosomal Hyal1, as evidenced by Pearson's correlation coefficient ($\rho = 0.88$, Fig 1E). We selected a transfectant line with expression of Hyal1WT that was comparable to the levels in the point mutant lines to perform all further functional characterizations.

Hyal1-containing exosomes are generated partially through an atypical autophagosomal route

Exosome biogenesis in tumor cells can occur through multiple routes, including the canonical inward budding of multivesicular bodies, as well as shedding from lysosomes and vesicles destined for lysosomal fusion [15, 20, 22, 23]. We had previously seen a strong impact of Hyal1 on vesicle trafficking that was dependent on autophagosome and lysosome activity, consistent with the primary cellular role of Hyal1 in lysosomal glycosaminoglycan breakdown and recycling. Therefore, we examined the relevance of autophagolysosomes to Hyal1 exosome production. Exosomes derived from tumor cell lines expressing catalytically active Hyal1WT-tdT and Hyal1Y202F-tdT contained significantly higher levels of LC3BII, a membrane-anchored protein component of autophagosomes, relative to those from the tdT or Hyal1E131Q-tdT lines. The addition of Bafilomycin A1 (BafA1), which prevents autophagosome-lysosome fusion and increases exosome shedding, increased the appearance of LC3BII in exosomes as expected (Fig 2A), except in Hyal1WT-tdT transfectants. Interestingly, BafA1 treatment also significantly increased the amount of Hyal1 per exosome (Fig 2B), and the greatest magnitude of the effect was associated with Hyal1WT-tdT. The level of Hyal1 per exosome was highest in those derived from Hyal1WT-tdT with and without chemical treatments, which suggests Hyal1 catalytic activity is required for its inclusion in exosomes shed by these routes, and that Hyal1 is included in exosomes generated by multiple mechanisms.

We further examined this using PC3 prostate carcinoma cells selected for stable knockdown of autophagosome biogenesis through shRNA targeting of the requisite component ATG5,

and quantifying endogenous Hyal1. ATG5 knockdown reduced exosome shedding in general, but also lowered the amount of LC3BII per exosome (Fig 2C), consistent with specific disruption of the autophagosomal route of exosome production. Importantly, the overall number of Hyal1-containing exosomes was reduced, and the amount of Hyal1 per exosome was also significantly lower, which confirms that Hyal1 can appear in exosomes via autophagosomes. Collectively, these results also confirm that endogenous Hyal1 traffics to endosomes by multiple routes similarly to the tdT fusion proteins, and that these processes are conserved between at least two prostate carcinoma cell lines.

Exosome production and quantity is robust and independent of Hyal1 overexpression

Next, we wanted to distinguish between delivery of Hyal1 into stromal cells via exosomes versus signaling events initiated by binding of exosomes to the cell surface. First, we confirmed that our exosomal preparations were of the expected morphology and purity by TEM (Fig 3A). We used nanoparticle tracking analysis (NTA) to quantify exosome numbers and average diameter, and determined that CD63 protein per million cells corresponded directly with the number of exosomes produced per million cells in each cell type (data not shown). On average, between 1.9 and 2.6 × 10^9 particles/million cells were produced by each of the clones, and the average particle diameter was 112 nm ± 11 nm (Fig 3B). NTA characterization of exosomes confirmed that CD63 normalization of samples for stromal cell treatment was appropriate for treatment normalization.

Exosomes secreted by prostate tumor cells deliver their contents directly to prostate stromal cells

By confocal fluorescence microscopy, we demonstrated that the exosomally-contained Hyal1-tdT fusion proteins were directly delivered to stromal cells. This was evident by the formation of red fluorescent puncta in our stromal cells following exposure to exosomes. The appearance of red fluorescence could be seen after approximately 15 minutes, confirming that exosomal contents were effectively taken up by stromal cells and delivered to vesicles within the stromal cells (Fig 3C).

Hyal1-containing exosomes do not affect the proliferation of prostate tumor or stromal cells

Exosomes produced by tumor cells induce proliferation of non-cancerous cell types [30–32, 34], and Hyal1 overexpression increases the cell-autonomous proliferation rate of tumor cell lines [35]. Therefore, we tested whether the exosomes produced by Hyal1-overexpressing tumor cells would enhance proliferation of either the parental tumor cell line or of prostate stromal cells. Exosomes isolated from 22Rv1 control (tdT), Hyal1WT-tdT, Hyal1E131Q-tdT, or Hyal1Y202F-tdT transfectants were applied to 22Rv1 prostate carcinoma cells daily for five days. No significant differences were observed in the proliferation rates regardless of treatment (Fig 4A). Identical results were obtained in similar experiments using tumor-derived exosomes to treat WPMY-1 prostate stromal cells. Like the 22Rv1 parental tumor cell line, WPMY-1 cells express relatively low Hyal1, low basal HA synthase, and produce low amounts of HA (not shown). These parameters did not change significantly in response to exosome treatments (not shown) and no significant difference in the proliferation rate was observed with treatment (Fig 4B). Thus, although there are differences in Hyal1 expression

in the exosomes produced by the tumor cells, these differences do not affect the proliferation of target cells.

Hyal1-containing exosomes enhance the migration of prostate stromal cells

Next, we tested whether tumor-derived exosome treatment could affect the motility of stromal cells. WPMY-1 cells were treated for 24 h with media containing isolated exosomes from each of the 22Rv1 transfectant conditioned media. Suspensions of each treated culture were placed in a modified Boyden chamber with type IV collagen in the lower wells. Significantly more WPMY-1 cell migration was observed when cells were treated with exosomes from tumor cells overexpressing catalytically active Hyal1-tdT (WT or Y202F) compared to cells treated with tdT control exosomes (Fig 5A, left). In contrast, cells treated with exosomes derived from Hyal1E131Q-tdT transfectants did not exhibit increased motility, indicating a requirement for Hyal1 catalytic activity. The level of exosomally-contained Hyal1 does not appear to affect the motility response beyond a reproducible threshold, with a maximal 2-fold increase observed with all exosome treatments. The importance of active Hyal1 in the exosomes was further validated using exosomes produced by PC3 lines (Fig 5A, right). PC3-pLKO control exosomes elicited a strong positive impact on stromal motility that was not induced by exposure to comparable numbers of exosomes containing lower Hyal1 due to ATG5 knockdown. Interestingly, when we treated the stromal cells with purified recombinant human Hyal1, we did not observe any differences in motility or proliferation, indicating that the context of Hyal1 delivery to the stromal cells (e.g., via exosomes) is critical to the response (Fig 5B, left). Different sizes of exogenously added HA representative of potential Hyal1-cleaved products also did not affect motility (Fig 5B, right), suggesting the exosomal Hyal1-induced motility response is elicited following target cell internalization of Hyal1-containing exosome contents and may not be strictly HA dependent.

Exposure to catalytically active Hyal1 in tumor-derived exosomes affects distribution but not expression of cell adhesion/motility receptors

We sought to understand the mechanism by which catalytically active Hyal1 leads to increased motility in prostate stromal cells. The increased expression of certain cell adhesion molecules is critical for induction of motility. We analyzed β1 integrin, β3 integrin, and N-cadherin/β-catenin levels from WCL of exosome-treated stromal cells by western blot. No significant changes in expression levels were observed (Fig 6A, 6B). We then performed cellular fractionation to determine whether increased β-catenin nuclear translocation was evident in exosome treated cells that demonstrated increased motility, but we could not discern any differences in levels of nuclear β-catenin between any of the exosomal treatment groups (Fig 6C). We further attempted to look for differences in cell surface chondroitin sulfate proteoglycans using western analysis with pan anti-chondroitin sulfate antibodies (not shown). Though we were able to visualize a heterogeneous distribution of many proteins on these westerns, we were not able to detect differences among exosome-exposed populations that were statistically significant. We also found no significant changes using flow cytometric quantification of integrins with multiple different monoclonal antibodies to compare exosome-treated and untreated cell surface expression (not shown).

We then used confocal immunofluorescence microscopy to compare β1 integrin staining intensity in intact and permeabilized 22Rv1 transfectant tumor cells, reasoning that subcellular distribution changes might be more subtle than bulk population analysis methods could effectively reveal. We found significantly increased plasma membrane (PM) β1 integrin in cells expressing Hyal1WT-tdT or Hyal1Y202F-tdT relative to those expressing the Hyal1E131Q-tdT mutant (Fig 6D). However, a similar microscopic analysis of stromal cells treated with Hyal1WT-tdT or Hyal1Y202F-tdT exosomes relative to those exposed to the tdT or Hyal1E131Q-tdT exosomes did not reveal significant differences in either PM or cytosolic β1 integrin. Instead, there was a notable increase in perinuclear β1 integrin staining in cells treated with Hyal1WT-tdT or Hyal1Y202F-tdT exosomes. When plotted as a ratio of PM to perinuclear integrin fraction, the result was a significant decrease relative to tdT or Hyal1E131Q-tdT exosome-treated cells (Fig 6E). Thus, the stable overexpression of active Hyal1 in tumor cells increased their motility by inducing a stable redistribution of β1 integrin that favored its cell surface presentation, while the delivery of catalytically active Hyal1-containing exosomes to stromal cells accelerated their motility by increasing the dynamic recycling of β1 integrin to and from the cell surface.

Catalytically active Hyal1 from tumor-derived exosomes stimulates stromal cell adhesion by increased activation of FAK

Altered dynamics in the membrane residence of β1 integrin are frequently accompanied by changes in adhesion and integrin-associated kinase activity, so we assayed adhesion of exosomally-treated stromal cells. We observed significant increases in adhesion of cells pre-treated with active Hyal1-containing exosomes, which corresponded directly with the trends observed for motility using the same exosome treatments (Fig 7A), supporting a role for the increased engagement of integrin receptors. To further test this, we assessed FAK activation, by detection of FAK phosphorylation at Tyr397. Phosphorylation of FAK was significantly elevated upon adhesion to Collagen IV, which followed the same trend with respect to catalytically active Hyal1-containing exosome treatments as did motility and adhesion (Fig 7B). We conclude that catalytically active Hyal1delivered via exosomes to stromal cells is required for motility and adhesion, and that it is not an upregulation of cell adhesion molecules, but instead an increased ability of the cells to engage these receptors that leads to the motile phenotype.

DISCUSSION

Exosomal transfer of proteins, RNA, and miRNA from cancer cells to non-cancerous cells has been shown to induce molecular changes in the recipient cells that can lead to their altered phenotypic properties, ultimately supportive of tumor growth. In this work, we have demonstrated that 22Rv1 prostate carcinoma cells overexpressing Hyal1WT or Hyal1 point mutants produce exosomes that contain Hyal1. Treatment of prostate stromal cells with tumor-derived exosomes containing catalytically active Hyal1 resulted in enhanced adhesion and motility of the stromal cells. Since this effect was not seen using exosomes released by cells expressing the catalytically inactive Hyal1E131Q-tdT mutant, the enhanced migratory phenotype must be dependent on intact Hyal1 activity. The catalytic activity is also important for the packaging of Hyal1 into exosomes. In addition, we find enriched release of

Hyal1WT-tdT via exosomes, while Hyal1E131Q-tdT is a more significant component of microvesicles, indicating that the catalytic activity of Hyal1 is important for its delivery into specific extracellular vesicles. This is consistent with previous results that demonstrate that the catalytic activity of Hyal1 dictates its trafficking itinerary in tumor cells [35].

Soluble rhHyal1 added directly to stromal cell cultures or suspensions did not impact their motility. There are several key differences between exosomal and soluble Hyal1 that could influence induction of motility. First, exosomally-contained Hyal1 is concentrated in exosomes and delivered directly into stromal cells, perhaps in a highly targeted manner, as suggested by the uptake studies. Second, a portion of the exosomally-contained Hyal1 is proteolytically cleaved, which may have the potential to elicit a different biological response than uncleaved rhHyal1, though no differences in intrinsic catalytic activity have been reported in studies in vitro [37, 38]. Third, it may be a combination of Hyal1 and HA contained in the exosome that leads to a maximal response. However, when we treated stromal cells with exogenous HA of different sizes, we did not observe any changes in motility. In addition, we have only detected very low levels of HA on exosomes from Hyal1 overexpressing clones, and they do not differ significantly between the exosomes collected from each clone.

Hyal1 also catalyzes hydrolysis of chondroitin sulfate, and can bind chondroitin sulfate proteoglycans such as integrins and other cell surface receptors, so its direct association is another means by which active Hyal1 may impact cell surface receptor engagement. For example, it is possible Hyal1 is adherent to the surface of exosomes and serves primarily to facilitate their cellular docking such that the exosomal contents are delivered more efficiently to the target cell. Upon internalization, changes in the vesicular microenvironment could potentially lead to Hyal1 dissociation and the exosomal remnants would then be available to engage in subsequent processes independently of Hyal1.

Specific cell adhesion molecules such as β1, β3, or β6 integrins [39–41] can be delivered via exosomes and shuttled directly into endosomal pathways of non-tumorigenic cell lines, leading to increased motility. We did not detect changes in levels of expression on tumor cells or on any exosome-treated stromal cells. Instead, the reorganization of integrins observed in stromal cells following active Hyal1-containing exosome treatment is consistent with previous reports in which apparent perinuclear β1 integrin accumulation is indicative of enhanced recycling rate and drives an accelerated rate of directional cell migration [42]. Moreover, this result further implicates Hyal1 in altered integrin engagement, possibly through induced vesicular recycling of integrins or via an inside-out signaling mechanism.

Exogenous treatment of 22Rv1 tumor cells overexpressing HA synthase with soluble rhHyal1 relieves their growth inhibition and restores their motility in culture through impacts on integrin-mediated adhesion [8, 9]. However, WPMY-1 cells do not have abundant surface HA in these studies and the cell proliferation is also not stimulated by Hyal1 treatment. We have further seen that Hyal1 uptake by tumor cells is enhanced by exogenously added HA in a manner dependent on its full HA binding potential (in a short time frame), and that vesicular trafficking of cell surface receptors is accelerated. Because of accelerated trafficking, there may be diminished “quality control” and a consequent loss of

accuracy in cargo loading of the exosomes in Hyal1-overexpressing cells that leads to aberrant responses in the target cells and/or enhanced docking or unloading of exosome cargoes in the target cells.

Using the Hyal1 mutant prostate cancer cell lines, we previously observed that a portion of catalytically active and internalized Hyal1was directed to lysosomes, and a significant portion of Hyal1 accumulated within autophagosomes upon BafA1 treatment [35]. It has been demonstrated that induction of autophagy can lead to increased exosome release, accompanied by increased presence of autophagosomal markers in these exosomes [43]. We showed here that Hyal1WT-tdT exosomes contain more of the autophagic marker LC3BII. It is possible that Hyal1 may play a direct role in the process of autophagy, and that vesicles released via this pathway could induce not only Hyal1-specific effects, but also autophagy-related effects. For example, it is known that autophagy promotes cell motility by regulating focal adhesion turnover [44–46].

We found that treatment of stromal cells with exosomes containing catalytically active Hyal1 increased their adherence to collagen IV and that this response occurred with increased activation of FAK by autophosphorylation of Y397, which is known to occur upon integrin engagement. This supports a mechanism whereby Hyal1-containing exosomes prime the cell for motility upon exposure to extracellular matrix substrates through pre-activation of integrins. As discussed above, this is consistent with the effect of Hyal1 overexpression in tumor cells, where catalytically active Hyal1 increases vesicular trafficking rate and alters presentation of cell surface receptors, since the trafficking rate is an important component of directional motility (reviewed by [47–49]). Clathrin-mediated endocytosis of β1 integrin is required at the cellular leading edge, coordinated with vesicle-mediated delivery of these and other surface proteins involved sustained directional motility to other regions of the cell [50]. Motility of the cell body requires both the formation and disassembly of nascent adhesions, and the rapid turnover of such adhesions increases speed of motility (reviewed by [51]). β1 integrin shuttling into filopodia may initiate focal contacts, and establish directional motility. We have observed that Hyal1WT-tdT and Hyal1Y202F-tdT overexpressing tumor cells initiate more numerous filopodia compared to tdT and Hyal1E131Q-tdT clones. It is possible that by direct transfer of Hyal1 via exosomes, a similar process is promoted in stromal fibroblasts that supports increased directional cell motility.

The appearance of Hyal1 in exosomes suggests a novel mechanism by which Hyal1 expression in tumor cells can influence cancer progression. 22Rv1 cells that overexpress Hyal1 are more rapidly metastatic than control cells [9]. Hyal1 is secreted as a soluble factor by the cell, and since its activity requires low pH, it could be locally active within acidic microenvironments at the tumor site. Presence of Hyal1 in exosomes implies that it could also be carried from the primary tumor site through the lymphatics or the circulation and arrive at target cells in remote tissues. In this way, a tumor overexpressing Hyal1 could initiate events to prepare tissues for metastasis. The exosome may fuse with the target cell membrane or be internalized by endocytosis. Hyal1 protein could facilitate docking and uptake of the vesicle and its contents, or it may increase proliferation and migration by producing active HA fragments. Since exosomes are more stable vesicles and travel farther through the circulation, while larger microvesicles are thought to carry out more local

communication, the impact of active Hyal1 protein could differ depending on whether it is secreted by exosomes or microvesicles. The content of the exosomes released by each cell type may facilitate long distance communication.

Further characterization of exosomes released by Hyal-overexpressing tumor cells is ongoing to determine whether Hyal1 modulates exosomal cargo sorting. For example, it will be important to characterize the cytokine expression in the prostate stromal cells treated with Hyal1-containing exosomes, as exosomes have previously been shown to upregulate pro-angiogenic cytokines [52]. Our results here suggest that the regulation of HA homeostasis via its synthesis and degradation enzymes can also have an effect on exosome production and content. Exosomes from prostate tumors could target nearby stromal cells within the prostate and induce pro-invasive phenotypes that would support cancer progression.

EXPERIMENTAL PROCEDURES

Cell culture

22Rv1 human prostate adenocarcinoma cells were purchased from ATCC and maintained in RPMI-1640 media containing 10% FBS. 22Rv1 cell lines stably expressing tdTomato (tdT, vector control), Hyal1WT-tdT, Hyal1E131Q-tdT, or Hyal1Y202F-tdT were selected as previously described [35] and maintained in RPMI-1640 containing 10% FBS and 1.5 mg/mL G418. WPMY-1 prostate stromal cells were purchased from ATCC, maintained in DMEM + 5% FBS and passaged as recommended by the vendor. PC3 human prostate carcinoma cells were selected for stable expression of pLKO (vector control) or one of two shRNA knockdown constructs targeting ATG5 (shATG5 #2 and shATG5 #5), and maintained in MEM containing 10% FBS, with non-essential amino acids, and sodium pyruvate.

Antibodies and reagents

Anti-Hyal1 rabbit polyclonal antibody was raised and characterized by our laboratory [35]. Anti-dsRed rabbit polyclonal was from Takara Bio USA, Inc. (Mountain View, CA). Anti-integrin β1 clone P5D2 was from Abcam (Cambridge, MA). Antibodies to ATG5 (rabbit polyclonal), LC3B (rabbit polyclonal), N-cadherin (13A9, mouse monoclonal), β-catenin (mouse monoclonal), FAK (rabbit polyclonal) and phospho-FAK (Tyr397, rabbit polyclonal) were from Cell Signaling Technology (Danvers, MA). Goat anti-rabbit IRDye800 and donkey anti-mouse IRDye800 were from Rockland Immunochemicals (Limerick, PA), and goat anti-mouse DyLight680 was from Thermo Fisher Scientific (Waltham, MA). Anti-CD63 mouse monoclonal and type IV mouse collagen were from BD Biosciences (San Jose, CA). All other reagents were from Thermo Fisher Scientific unless noted otherwise.

Isolation and characterization of exosomes

Tumor cells to be used for exosome isolation were cultured to 70% confluence in standard conditions. Media were then replaced with RPMI-1640 containing 10% low IgG FBS from which bovine exosomes had been removed by centrifugation at 100,000g for 12 h (exosome-depleted media). After 48 h, exosomes were harvested from the conditioned media by differential centrifugation at 4°C as follows. First, cells were pelleted and removed by 10

min at 200g; additional cells and debris were removed by 10 min at 2000g; microvesicles (diameter >150 nm) were depleted by centrifugation for 30 min at 10,000g; and finally, the resultant supernatant was centrifuged at 100,000g for 2 h to pellet exosomes. For proliferation and motility assays, the exosome pellet was resuspended in serum free DMEM, sterilized by passing through a 0.22μm syringe filter, and stored at −80°C. For quantification of protein expression in exosomes, the exosome pellet was resuspended in RIPA buffer supplemented with 1X protease inhibitor cocktail. Exosome identity, yield and quantity were confirmed for each initial preparation by transmission electron microscopy (TEM), western analysis of CD63 normalized to protein content, and nanoparticle tracking analysis (NTA). Exosome pellets to be imaged by TEM were resuspended in ultrapure water and prepared with a 2% uranyl acetate negative stain. Exosomes were imaged at 30,000X magnification with a Hitachi H7500 TEM operating at 80KV. Exosomes for NTA were diluted 500–2000-fold in ultrapure water and analyzed with a Malvern Nanosight NS300 using NTA software 3.0.

Chemical inhibitor treatments

Tumor cell stable lines were seeded overnight at equivalent cell density in RPMI-1640 with 10% exosome-depleted FBS. Cells were treated with Bafilomycin A1 at a final concentration of 5 nM for 48 h. Control plates received vehicle (DMSO) for the duration of the assay. Conditioned media were harvested from all plates 72 h after initial seeding. Exosomes were isolated, lysed, and analyzed by western blot as described.

Exosome treatments

All exosome treatment volumes were determined by nanoparticle tracking assay and relative CD63 expression levels and adjusted to deliver equal numbers of exosomes. We titrated the amount of Hyal1WT present in exosomes on the basis of Hyal1 protein expression in the exosomes as measured by western blot, and also based on Hyal1 catalytic activity measured in sonicated exosome preparations. We confirmed that the amount of exosomal Hyal1 administered to cells was consistent with the amount of exogenously added recombinant Hyal1, and that our administered doses reflected clinically relevant levels reported in resected tumor specimens. Prior to treatment, WPMY-1 cells were seeded for 24 h in exosome-depleted media. Media were removed and replaced with serum free DMEM ± equal numbers of exosomes. Cells were incubated with exosomes for 24 h, followed by lysis for western analysis, or functional assays for motility, adhesion, and FAK activation. Internalization of exosomal content was confirmed by confocal fluorescence microscopy, monitoring intracellular tdTomato signal accumulation following exosome addition to WPMY-1 cells cultured on glass bottom tissue culture dishes overnight. Z-series images were collected 15 minutes after exosome addition using an Olympus FV500 inverted confocal microscope, and the 543 nm excitation laser.

FAK Activation

Phosphorylation of FAK was assayed in exosome-treated cells following exposure to collagen. Prior to the assay, 12-well plates were incubated overnight at 37°C with mouse collagen IV (20μg/mL in DPBS), blocked with BSA (5% in Dulbecco's PBS) for 1 h at room temperature, and washed with DPBS. Exosome-treated WPMY-1 cells were trypsin-

released and seeded onto the collagen-coated plates for 2 h at 37°C in a humidified CO_2 incubator. Non-adherent cells were removed by gentle washing with prewarmed DPBS. Remaining cells were lysed with RIPA buffer containing 1X protease inhibitor cocktail and 1μg/mL sodium orthovanadate. Lysates were snap frozen in liquid nitrogen and stored at −80°C until protein quantification by BCA and western analysis. Activation of FAK was plotted as the ratio of phosphorylated to total FAK.

Western analysis

All whole cell lysates (WCL) for western analysis were prepared in RIPA lysis buffer with protease inhibitor cocktail and separated by reducing or non-reducing SDS-PAGE as recommended by the antibody vendors. For non-reducing gels, WCL and conditioned media fractions were mixed with Laemmli buffer and incubated at 37°C for 30 min prior to SDS-PAGE. For reducing gels, samples were mixed with Laemmli buffer containing 5% β-mercaptoethanol and subsequently handled similarly. Protein content of both WCL and conditioned media fractions was assessed by BCA assay and equal amounts of protein were compared for each type of sample (30μg for WCL and 40μg for exosome/conditioned media samples). After electrophoresis, proteins were transferred to PDVF membranes, blocked in PBS containing 0.1% Tween-20 (PBST) and 5% milk, and incubated with primary antibody in PBST with 5% milk for 2 h at room temperature. Membranes were washed in PBST, incubated with appropriate secondary antibody, imaged using the LI-COR Odyssey and analyzed with Image Studio Lite. WCL of overexpressing cells were used to confirm specificity of the dsRed antibody for Hyal1-containing bands by first probing with anti-Hyal1 and then stripping and reprobing for dsRed. Blots originally imaged for pFAK were stripped and reprobed with FAK antibody.

Cell proliferation

Proliferation was measured with WST-1 reagent according to manufacturer instructions (Roche Life Science). Briefly, cells were seeded in a 96 well plate at 5000 cells per well. The medium was replaced 24 h after seeding and subsequently every 48 h until the end of the assay with either snap frozen fresh medium (control) or medium containing snap frozen resuspended exosomes. Absorbance at 450 nm was measured daily in triplicate wells following incubation with WST-1.

Cell motility

Motility was measured in a 48-well chemotaxis chamber with 8 μm pore sized polycarbonate membranes (Neuro Probe Inc., Gaithersburg, MD). Type IV mouse collagen (25 μg/mL in serum-free DMEM) was used as the chemoattractant in the lower wells. Cells previously treated with and without exosome containing media were suspended and placed in the upper wells (25,000 per well in serum-free medium). The chamber was incubated in a humidified 5% CO_2 incubator at 37 °C for 6 h. After incubation, the membranes were developed using the Diff Quik Stain Kit (VWR International, Batavia, IL). Unmigrated cells were removed with a cotton swab. The membrane was mounted on a glass slide with Fluoromount-G (Southern Biotech Associates, Inc., Birmingham, AL). Migrated cells were manually counted at 40x magnification on an inverted microscope. The assay was

reproduced at least three times with three different exosome preparations for each tumor line.

Adhesion

Microwell plates were precoated with 20 μg/mL mouse collagen IV overnight at 37°C, blocked with 5% BSA for 1 h at room temperature, and washed with DPBS. Exosome-treated WPMY-1 cells were trypsinized, counted, and labeled with calcein-AM (25μM, 1×10^5 cells/mL in serum free DMEM) 20 min at 37°C. Labeled cells were washed with DPBS, resuspended at 10^4 cells/mL in serum free DMEM, and 0.1 ml/well was applied to quadruplicate wells of the precoated 96-well plates. After 30 minutes, non-adherent cells were removed by two gentle washes with serum free DMEM. Cells were lysed by adding 100 μL of 0.02N HCl and 0.1% SDS and the fraction of adherent cells was quantified in a fluorescence plate reader. Labeled WPMY-1 cells were used concurrently to generate a standard curve of 5%–100% input cell numbers. Fluorescence intensities were used to interpolate percentage of adhesion from the standard curve.

Acknowledgments

The authors thank Dr. Joe Barycki and members of the Simpson lab for critical input and suggestions. These studies were supported by NIH R01 CA165574 (to MAS). Nanoparticle tracking analysis was completed with assistance from the University of Nebraska Biomedical and Obesity Research Core, funded by NIH P20 GM104320. Transmission electron microscopy was assisted by Han Chen and the University of Nebraska Morrison Microscopy Facility.

Abbreviations

HA	hyaluronan
FAK	focal adhesion kinase
PM	plasma membrane
NTA	nanoparticle tracking analysis

LITERATURE CITED

1. Aaltomaa S, Lipponen P, Tammi R, Tammi M, Viitanen J, Kankkunen JP, Kosma VM. Strong Stromal Hyaluronan Expression Is Associated with PSA Recurrence in Local Prostate Cancer. Urol Int. 69(4)2002; :266–72. [PubMed: 12444281]
2. Ekici S, Ayhan A, Kendi S, Ozen H. Determination of prognosis in patients with prostate cancer treated with radical prostatectomy: prognostic value of CD44v6 score. The Journal of urology. 167(5)2002; :2037–41. [PubMed: 11956433]
3. McAtee CO, Barycki JJ, Simpson MA. Emerging roles for hyaluronidase in cancer metastasis and therapy. Advances in cancer research. 1232014; :1–34. [PubMed: 25081524]
4. Posey JT, Soloway MS, Ekici S, Sofer M, Civantos F, Duncan RC, Lokeshwar VB. Evaluation of the prognostic potential of hyaluronic acid and hyaluronidase (HYAL1) for prostate cancer. Cancer research. 63(10)2003; :2638–44. [PubMed: 12750291]
5. Simpson MA, Lokeshwar VB. Hyaluronan and hyaluronidase in genitourinary tumors. Front Biosci. 132008; :5664–80. [PubMed: 18508614]
6. Toole BP. Hyaluronan promotes the malignant phenotype. Glycobiology. 12(3)2002; :37R–42R.

7. Toole BP. Hyaluronan: from extracellular glue to pericellular cue. Nat Rev Cancer. 4(7)2004; :528–39. [PubMed: 15229478]
8. Bharadwaj AG, Goodrich NP, McAtee CO, Haferbier K, Oakley GG, Wahl JK 3rd, Simpson MA. Hyaluronan suppresses prostate tumor cell proliferation through diminished expression of N-cadherin and aberrant growth factor receptor signaling. Experimental cell research. 317(8)2011; :1214–25. [PubMed: 21315068]
9. Bharadwaj AG, Kovar JL, Loughman E, Elowsky C, Oakley GG, Simpson MA. Spontaneous metastasis of prostate cancer is promoted by excess hyaluronan synthesis and processing. The American journal of pathology. 174(3)2009; :1027–36. [PubMed: 19218337]
10. Kovar JL, Johnson MA, Volcheck WM, Chen J, Simpson MA. Hyaluronidase expression induces prostate tumor metastasis in an orthotopic mouse model. The American journal of pathology. 169(4)2006; :1415–26. [PubMed: 17003496]
11. Lokeshwar VB, Cerwinka WH, Isoyama T, Lokeshwar BL. HYAL1 hyaluronidase in prostate cancer: a tumor promoter and suppressor. Cancer research. 65(17)2005; :7782–9. [PubMed: 16140946]
12. Mahaffey CL, Mummert ME. Hyaluronan synthesis is required for IL-2-mediated T cell proliferation. J Immunol. 179(12)2007; :8191–9. [PubMed: 18056362]
13. Zhao N, Wang X, Qin L, Guo Z, Li D. Effect of molecular weight and concentration of hyaluronan on cell proliferation and osteogenic differentiation in vitro. Biochemical and biophysical research communications. 465(3)2015; :569–74. [PubMed: 26284973]
14. Arenaccio C, Federico M. The Multifaceted Functions of Exosomes in Health and Disease: An Overview. Adv Exp Med Biol. 9982017; :3–19. [PubMed: 28936729]
15. Hessvik NP, Llorente A. Current knowledge on exosome biogenesis and release. Cellular and molecular life sciences : CMLS. 2017
16. Taylor DD, Gercel-Taylor C. MicroRNA signatures of tumor-derived exosomes as diagnostic biomarkers of ovarian cancer. Gynecologic oncology. 110(1)2008; :13–21. [PubMed: 18589210]
17. Logozzi M, De Milito A, Lugini L, Borghi M, Calabro L, Spada M, Perdicchio M, Marino ML, Federici C, Iessi E, Brambilla D, Venturi G, Lozupone F, Santinami M, Huber V, Maio M, Rivoltini L, Fais S. High levels of exosomes expressing CD63 and caveolin-1 in plasma of melanoma patients. PloS one. 4(4)2009; :e5219. [PubMed: 19381331]
18. Kahlert C, Kalluri R. Exosomes in tumor microenvironment influence cancer progression and metastasis. Journal of molecular medicine. 91(4)2013; :431–7. [PubMed: 23519402]
19. Ruivo CF, Adem B, Silva M, Melo SA. The Biology of Cancer Exosomes: Insights and New Perspectives. Cancer research. 77(23)2017; :6480–6488. [PubMed: 29162616]
20. Stoorvogel W, Kleijmeer MJ, Geuze HJ, Raposo G. The biogenesis and functions of exosomes. Traffic. 3(5)2002; :321–30. [PubMed: 11967126]
21. Trajkovic K, Hsu C, Chiantia S, Rajendran L, Wenzel D, Wieland F, Schwille P, Brugger B, Simons M. Ceramide triggers budding of exosome vesicles into multivesicular endosomes. Science. 319(5867)2008; :1244–7. [PubMed: 18309083]
22. Machado E, White-Gilbertson S, van de Vlekkert D, Janke L, Moshiach S, Campos Y, Finkelstein D, Gomero E, Mosca R, Qiu X, Morton CL, Annunziata I, d'Azzo A. Regulated lysosomal exocytosis mediates cancer progression. Science advances. 1(11)2015; :e1500603. [PubMed: 26824057]
23. Soto-Heredero G, Baixauli F, Mittelbrunn M. Interorganelle Communication between Mitochondria and the Endolysosomal System. Frontiers in cell and developmental biology. 52017; :95. [PubMed: 29164114]
24. Zhang J, Li S, Li L, Li M, Guo C, Yao J, Mi S. Exosome and exosomal microRNA: trafficking, sorting, and function. Genomics, proteomics & bioinformatics. 13(1)2015; :17–24.
25. Peinado H, Aleckovic M, Lavotshkin S, Matei I, Costa-Silva B, Moreno-Bueno G, Hergueta-Redondo M, Williams C, Garcia-Santos G, Ghajar C, Nitadori-Hoshino A, Hoffman C, Badal K, Garcia BA, Callahan MK, Yuan J, Martins VR, Skog J, Kaplan RN, Brady MS, Wolchok JD, Chapman PB, Kang Y, Bromberg J, Lyden D. Melanoma exosomes educate bone marrow progenitor cells toward a pro-metastatic phenotype through MET. Nature medicine. 18(6)2012; :883–91.

26. Peinado H, Lavotshkin S, Lyden D. The secreted factors responsible for pre-metastatic niche formation: old sayings and new thoughts. Seminars in cancer biology. 21(2)2011; :139–46. [PubMed: 21251983]
27. Ramteke A, Ting H, Agarwal C, Mateen S, Somasagara R, Hussain A, Graner M, Frederick B, Agarwal R, Deep G. Exosomes secreted under hypoxia enhance invasiveness and stemness of prostate cancer cells by targeting adherens junction molecules. Molecular carcinogenesis. 54(7)2015; :554–65. [PubMed: 24347249]
28. Erez N, Truitt M, Olson P, Arron ST, Hanahan D. Cancer-Associated Fibroblasts Are Activated in Incipient Neoplasia to Orchestrate Tumor-Promoting Inflammation in an NF-kappaB-Dependent Manner. Cancer cell. 17(2)2010; :135–47. [PubMed: 20138012]
29. Tuxhorn JA, Ayala GE, Smith MJ, Smith VC, Dang TD, Rowley DR. Reactive stroma in human prostate cancer: induction of myofibroblast phenotype and extracellular matrix remodeling. Clinical cancer research : an official journal of the American Association for Cancer Research. 8(9)2002; :2912–23. [PubMed: 12231536]
30. Gutkin A, Uziel O, Beery E, Nordenberg J, Pinchasi M, Goldvaser H, Henick S, Goldberg M, Lahav M. Tumor cells derived exosomes contain hTERT mRNA and transform nonmalignant fibroblasts into telomerase positive cells. Oncotarget. 7(37)2016; :59173–59188. [PubMed: 27385095]
31. Paggetti J, Haderk F, Seiffert M, Janji B, Distler U, Ammerlaan W, Kim YJ, Adam J, Lichter P, Solary E, Berchem G, Moussay E. Exosomes released by chronic lymphocytic leukemia cells induce the transition of stromal cells into cancer-associated fibroblasts. Blood. 126(9)2015; :1106–17. [PubMed: 26100252]
32. Webber JP, Spary LK, Sanders AJ, Chowdhury R, Jiang WG, Steadman R, Wymant J, Jones AT, Kynaston H, Mason MD, Tabi Z, Clayton A. Differentiation of tumour-promoting stromal myofibroblasts by cancer exosomes. Oncogene. 2014
33. Thompson CA, Purushothaman A, Ramani VC, Vlodavsky I, Sanderson RD. Heparanase regulates secretion, composition, and function of tumor cell-derived exosomes. The Journal of biological chemistry. 288(14)2013; :10093–9. [PubMed: 23430739]
34. Webber J, Steadman R, Mason MD, Tabi Z, Clayton A. Cancer exosomes trigger fibroblast to myofibroblast differentiation. Cancer research. 70(23)2010; :9621–30. [PubMed: 21098712]
35. McAtee CO, Berkebile AR, Elowsky CG, Fangman T, Barycki JJ, Wahl JK 3rd, Khalimonchuk O, Naslavsky N, Caplan S, Simpson MA. Hyaluronidase Hyal1 Increases Tumor Cell Proliferation and Motility through Accelerated Vesicle Trafficking. The Journal of biological chemistry. 290(21)2015; :13144–56. [PubMed: 25855794]
36. Escola JM, Kleijmeer MJ, Stoorvogel W, Griffith JM, Yoshie O, Geuze HJ. Selective enrichment of tetraspan proteins on the internal vesicles of multivesicular endosomes and on exosomes secreted by human B-lymphocytes. The Journal of biological chemistry. 273(32)1998; :20121–7. [PubMed: 9685355]
37. Csoka AB, Frost GI, Wong T, Stern R. Purification and microsequencing of hyaluronidase isozymes from human urine. FEBS letters. 417(3)1997; :307–10. [PubMed: 9409739]
38. Zhang L, Bharadwaj AG, Casper A, Barkley J, Barycki JJ, Simpson MA. Hyaluronidase activity of human Hyal1 requires active site acidic and tyrosine residues. The Journal of biological chemistry. 284(14)2009; :9433–42. [PubMed: 19201751]
39. Fedele C, Singh A, Zerlanko BJ, Iozzo RV, Languino LR. The alphavbeta6 integrin is transferred intercellularly via exosomes. The Journal of biological chemistry. 290(8)2015; :4545–51. [PubMed: 25568317]
40. Singh A, Fedele C, Lu H, Nevalainen MT, Keen JH, Languino LR. Exosome-mediated Transfer of alphavbeta3 Integrin from Tumorigenic to Nontumorigenic Cells Promotes a Migratory Phenotype. Molecular cancer research : MCR. 14(11)2016; :1136–1146. [PubMed: 27439335]
41. Hurwitz SN, Rider MA, Bundy JL, Liu X, Singh RK, Meckes DG Jr. Proteomic profiling of NCI-60 extracellular vesicles uncovers common protein cargo and cancer type-specific biomarkers. Oncotarget. 7(52)2016; :86999–87015. [PubMed: 27894104]

42. Kabir-Salmani M, Shiokawa S, Akimoto Y, Sakai K, Iwashita M. The role of alpha(5)beta(1)-integrin in the IGF-I-induced migration of extravillous trophoblast cells during the process of implantation. Molecular human reproduction. 10(2)2004; :91–7. [PubMed: 14742693]
43. Kumar D, Gupta D, Shankar S, Srivastava RK. Biomolecular characterization of exosomes released from cancer stem cells: Possible implications for biomarker and treatment of cancer. Oncotarget. 6(5)2015; :3280–91. [PubMed: 25682864]
44. Kenific CM, Wittmann T, Debnath J. Autophagy in adhesion and migration. J Cell Sci. 129(20)2016; :3685–3693. [PubMed: 27672021]
45. Mowers EE, Sharifi MN, Macleod KF. Novel insights into how autophagy regulates tumor cell motility. Autophagy. 12(9)2016; :1679–80. [PubMed: 27439889]
46. Xu Z, Klionsky DJ. Autophagy promotes cell motility by driving focal adhesion turnover. Autophagy. 12(10)2016; :1685–1686. [PubMed: 27483986]
47. Fletcher SJ, Rappoport JZ. The role of vesicle trafficking in epithelial cell motility. Biochemical Society transactions. 37(Pt 5)2009; :1072–6. [PubMed: 19754454]
48. Goldenring JR. A central role for vesicle trafficking in epithelial neoplasia: intracellular highways to carcinogenesis. Nat Rev Cancer. 13(11)2013; :813–20. [PubMed: 24108097]
49. Ridley AJ. Life at the leading edge. Cell. 145(7)2011; :1012–22. [PubMed: 21703446]
50. Chao WT, Kunz J. Focal adhesion disassembly requires clathrin-dependent endocytosis of integrins. FEBS letters. 583(8)2009; :1337–43. [PubMed: 19306879]
51. Huttenlocher A, Horwitz AR. Integrins in cell migration. Cold Spring Harbor perspectives in biology. 3(9)2011; :a005074. [PubMed: 21885598]
52. Hood JL, Pan H, Lanza GM, Wickline SA. I. Consortium for Translational Research in Advanced, Nanomedicine, Paracrine induction of endothelium by tumor exosomes. Lab Invest. 89(11)2009; : 1317–28. [PubMed: 19786948]

Highlights

- The hyaluronan-catabolizing enzyme Hyal1 is abundant in exosomes secreted by tumor cells.
- Packaging of Hyal1 in these vesicles occurs in part through an atypical autophagosomal and/or lysosomal route, in a manner dependent on its catalytic activity.
- Treatment of prostate stromal cells with exosomes from tumor cells expressing active Hyal1 significantly increases stromal cell motility.
- Tumor Hyal1-containing exosomes induce dynamic reorganization of β1 integrin from plasma membrane residence to a perinuclear recycling complex within the stromal cells, accompanied by increased FAK phosphorylation.
- These results are the first to implicate tumor Hyal1 in microenvironment reorganization via a novel exosomal delivery mechanism and to demonstrate a direct impact of Hyal1 exosomes on stromal cell behavior.

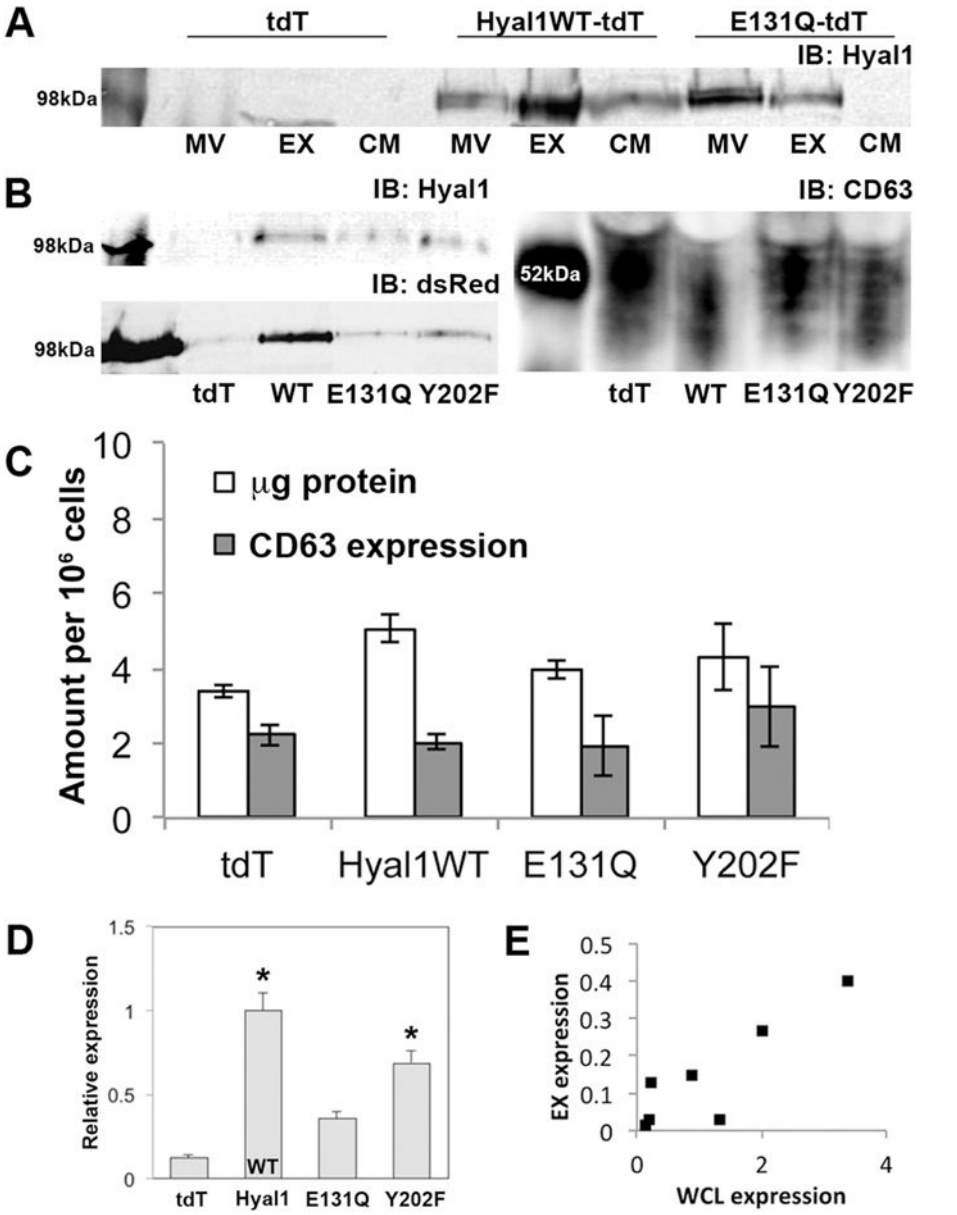

Figure 1. Exosomes secreted by prostate tumor cells contain catalytically active Hyal1

Conditioned media were collected from stable 22Rv1 transfectants expressing tdTomato (tdT, vector control), or the indicated Hyal1 construct, after culturing in exosome-depleted media for 48 hours. Large microvesicle (MV) and exosome (EX) fractions were prepared from conditioned media by differential centrifugation. (A) Equal amounts of protein from each fraction were immunoblotted for Hyal1. CM indicates concentrated media fractions following exosome centrifugation. (B) Exosomal fractions were immunoblotted for Hyal1 (upper left), dsRed (lower left), and CD63 (right). Expected band size is ≈100 kDa for Hyal1-tdT fusion proteins. Expected band ranges from 42–53 kDa for CD63. One representative analysis series is shown from a total of >4 separate exosome preparations. (C) Comparison of exosomal yield per million cells. Protein concentration was determined by BCA assay, CD63 expression was estimated by western blot. Mean ± SEM of three

exosomal preparations for each transfectant are presented. No significant differences were observed between these samples. (D) Relative amount of Hyal1 in the exosomal fraction of each cell line was compared by plotting the ratio of dsRed in a region of interest at 100kDa to CD63 in the western analysis. At least four separate preparations of exosomes from each line were analyzed. Mean ± SEM is plotted; *$p<0.05$ relative to the E131Q-tdT mutant. (E) Pearson's correlation coefficient was calculated for Hyal1WT-tdT expression in exosomes versus whole cell lysates. $\rho=0.88$.

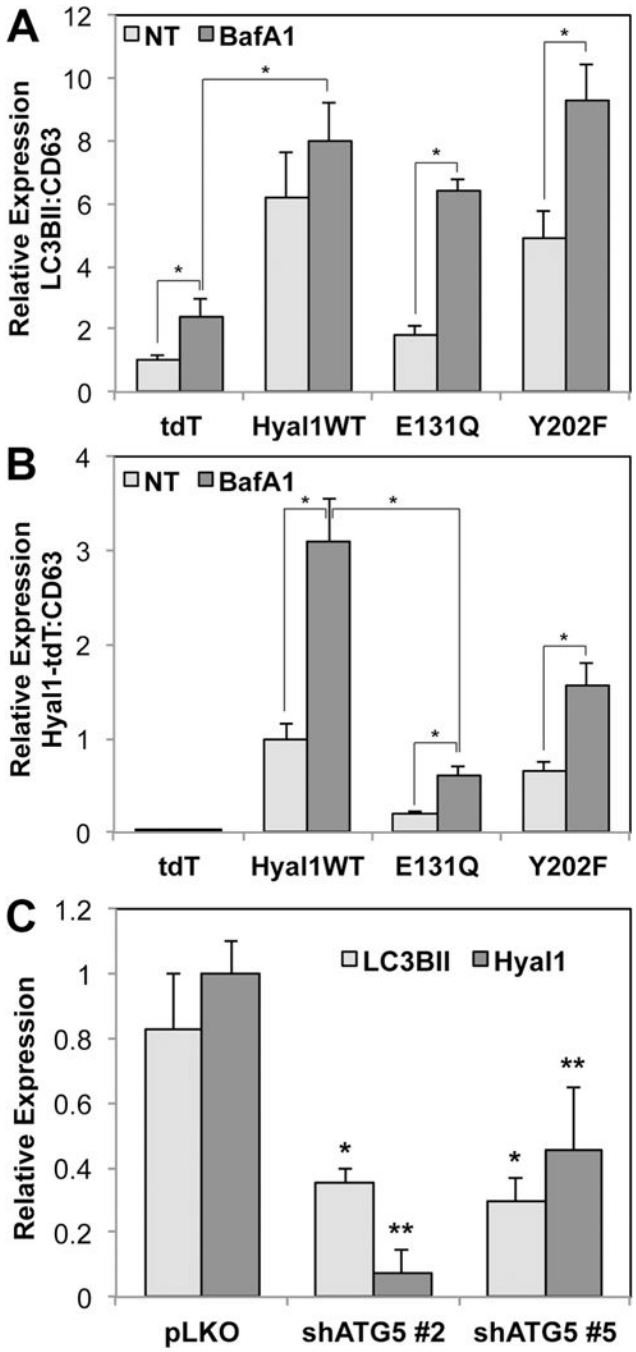

Figure 2. Hyal1-containing exosomes are shed partially by an autophagosomal route

(A, B) Hyal1 expression increases exosomal content of LC3BII and Hyal1-containing exosome secretion is stimulated by Bafilomycin A1. Exosome fractions from 22Rv1 cells stably expressing tdT, Hyal1WT-tdT, Hyal1E131Q-tdT, or Hyal1Y202F-tdT were analyzed by western blot for CD63, Hyal1-tdT, and the autophagic marker LC3BII. Triplicates of each blot were quantified to compare relative amounts of LC3BII, normalized to CD63 (A), or Hyal1:CD63 (B) for each of the transfectant lines. Mean ± SEM is plotted; * $p<0.05$. (C) ATG5 knockdown diminishes exosome shedding, extracellular Hyal1, and Hyal1-positive

exosomes, and significantly reduces exosomal Hyal1 content (normalized to CD63). Using PC3 cells selected for vector (pLKO) or ATG5 shRNA (two constructs, #2 and #5), exosomes were analyzed by western blot for CD63, LC3BII, and endogenous Hyal1. Levels of LC3BII and Hyal1 were normalized to CD63 in each preparation. Mean ± SEM is plotted; * $p<0.05$ for LC3BII expression relative to pLKO; ** $p<0.05$ for Hyal1 expression relative to pLKO.

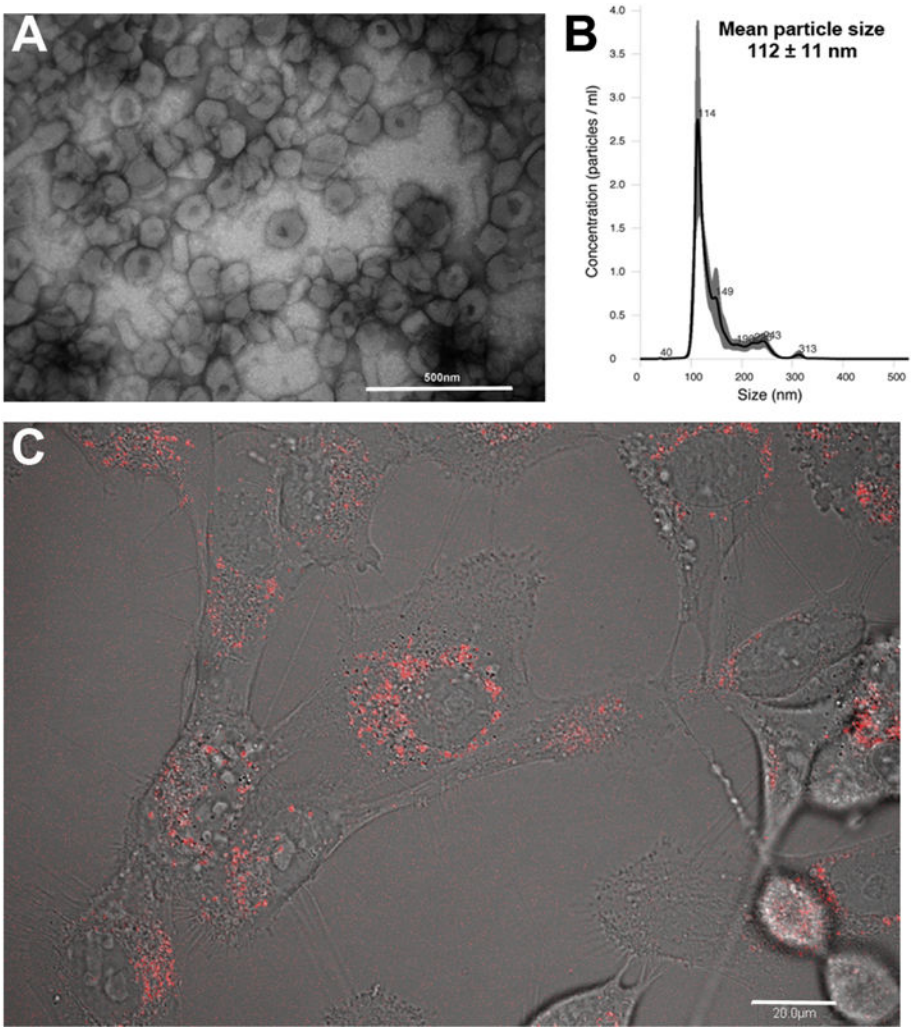

Figure 3. Tumor exosome contents are internalized by WPMY-1 prostate stromal fibroblasts

(A) Exosomes were isolated from 22Rv1 Hyal1WT-tdT transfected cell conditioned medium and imaged by TEM to confirm their correct size and morphology (scale bar is 500 nm). (B) Exosomes were characterized by nanoparticle tracking analysis to obtain numbers, average size, and size homogeneity. (C) WPMY-1 cells were seeded overnight on glass bottom tissue culture dishes, exposed to exosomes for 15 minutes, and imaged by fluorescence confocal microscopy to visualize and confirm tdT reporter internalization. Red fluorescent signal was visible in intracellular punctate structures consistent with endosomally internalized vesicles (scale bar is 20 μm, a single subsurface z-section is shown).

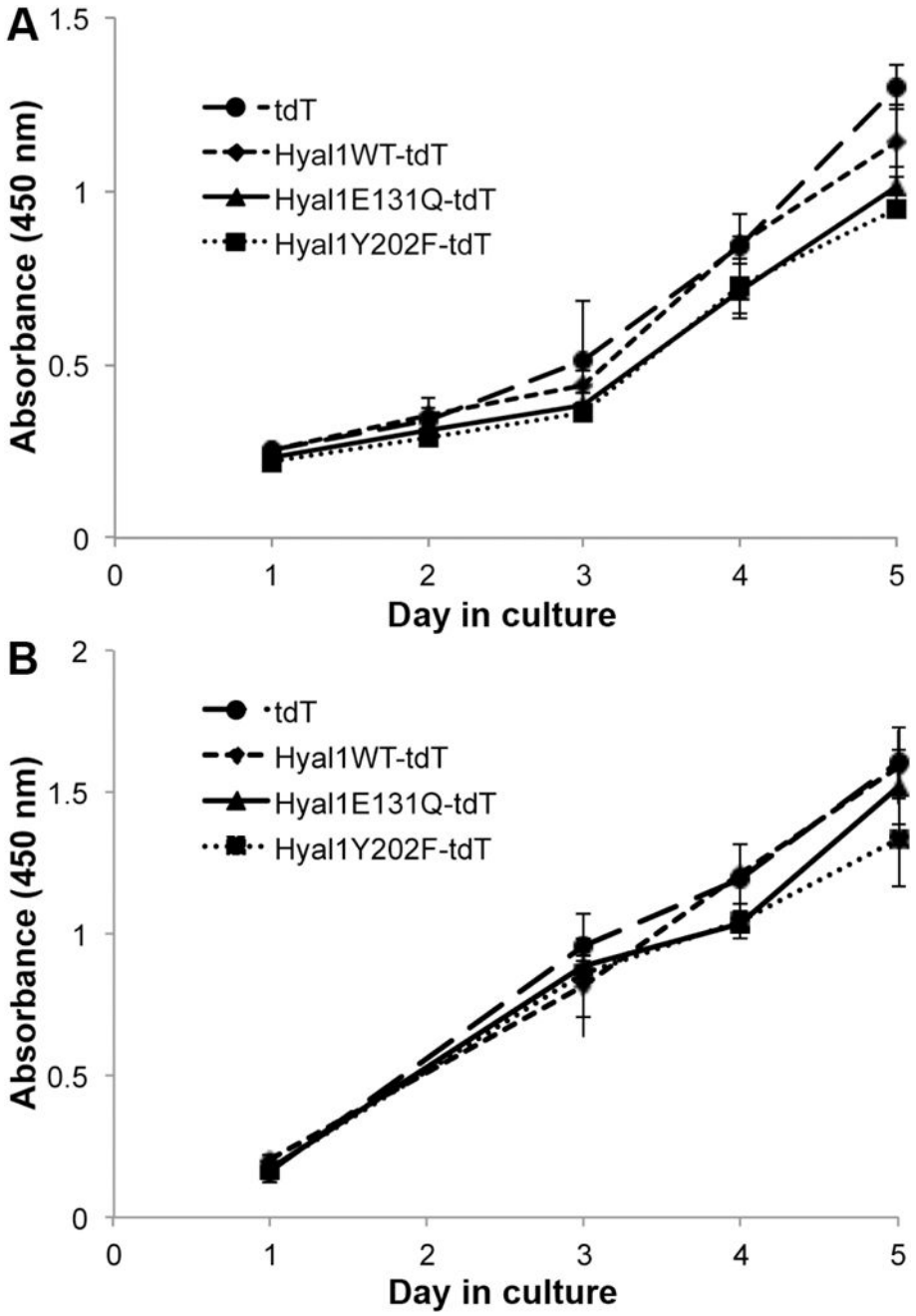

Figure 4. Proliferation of tumor and stromal cells is not affected by treatment with exosomes containing Hyal1

Tumor cells (22Rv1, A) or stromal cells (WPMY-1, B) were seeded at equal density in 96 well plates (day "0"). Proliferation was measured daily, or as indicated, by absorbance upon treatment with WST-1. Media were replaced on day 1 and every other day thereafter with RPMI + 5% FBS that contained isolated exosomes from the indicated tumor transfectant lines. Each condition was monitored in quadruplicate wells. Mean ± SEM is plotted for each day. No significant differences were observed among treatments.

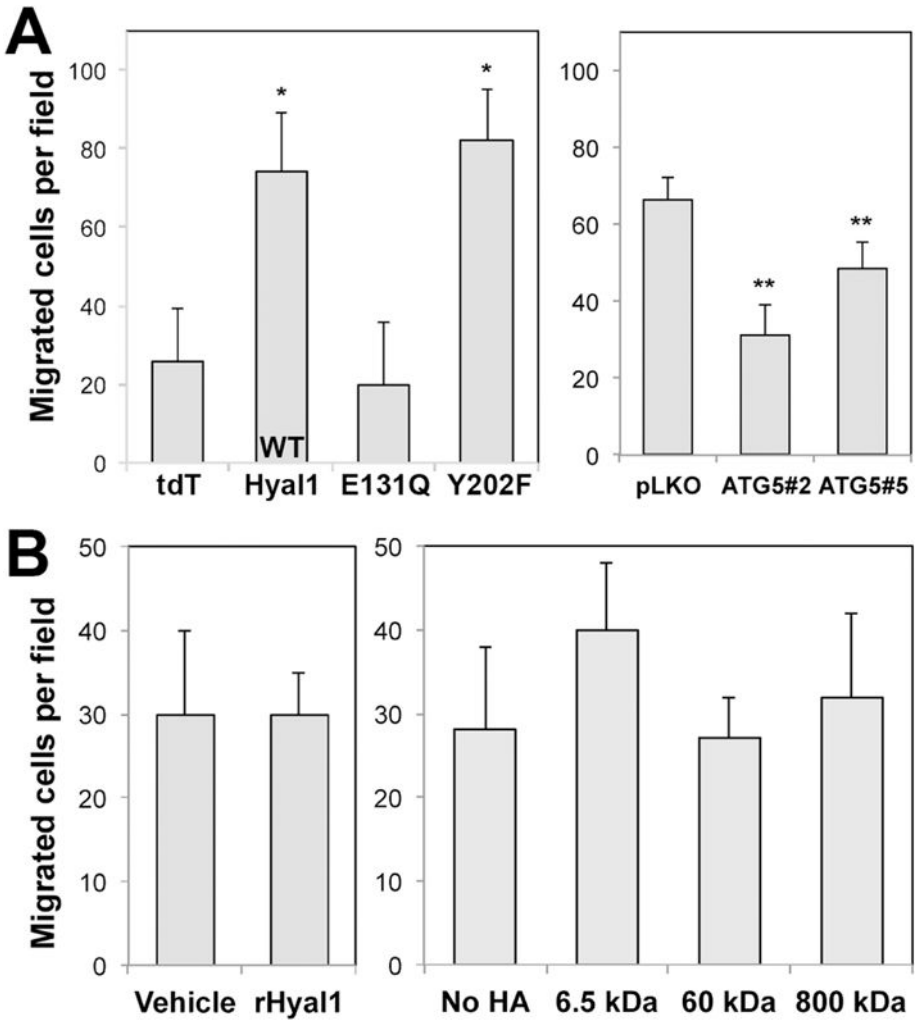

Figure 5. Tumor-derived exosomes containing catalytically active Hyal1WT stimulate prostate stromal cell motility

(A) WPMY-1 prostate stromal fibroblasts were treated for 24 h with exosome-depleted media to which aliquots of isolated exosomes from the indicated tumor cell lines were added (22Rv1 exosomal effects shown at left, PC3 effects at right). Migration of exosome-treated or untreated WPMY-1 cells to type IV collagen was compared using a modified Boyden chamber assay. Mean number of cells migrated per field is plotted ± SEM for triplicate wells; * $p<0.05$ relative to the tdT exosome control treatment; ** $p<0.05$ relative to the pLKO exosome control treatment. (B) Purified recombinant Hyal1 protein (left) or exogenous HA of different sizes (right) does not affect WPMY-1 motility. Stromal cells were treated with 10 ng/ml rhHyal1 or 10 μg/mL of the indicated size of HA in SFM for 24 h before chemotaxis assay. No significant differences were observed among these treatments.

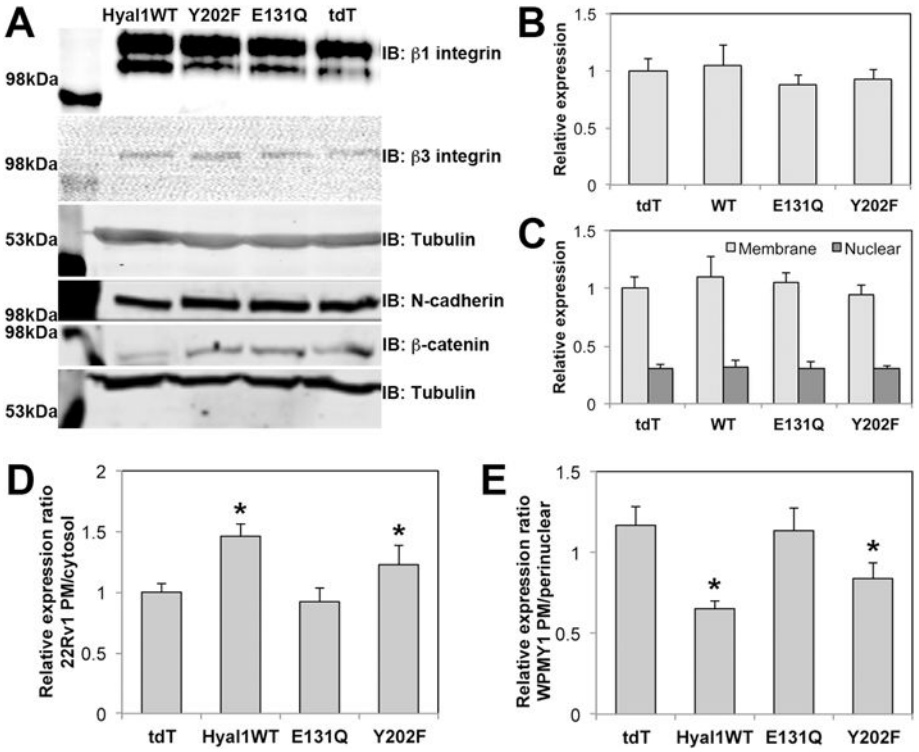

Figure 6.

Exosomes containing active Hyal1 do not affect stromal cell expression of specific motility receptors, but membrane residence of β1 integrin is altered. Stromal cells were treated with exosomes normalized to CD63 expression for 24 hours in SFM. (A) Whole cell lysates of treated cells were analyzed for β1 integrin, β3 integrin, N-cadherin, or β-catenin expression. (B) Plasma membrane enriched fractions were analyzed for N-cadherin expression. (C) Exosome-treated cells were fractionated into membrane and nuclear compartments and analyzed by western blot for β-catenin. (D) Cell surface and cytosolic β1 integrin was imaged by immunofluorescence confocal microscopy of intact and permeabilized 22Rv1 tumor cell transfectant lines cells, respectively (n=10 per condition), quantified in Image J, and plotted as a ratio for surface to cytosol. (E) Cell surface versus cytosolic β1 integrin was imaged by immunofluorescence confocal microscopy of intact and permeabilized exosome-treated stromal cells, respectively (n=20 per condition), quantified in Image J, and plotted as a ratio for surface to perinuclear staining intensity. In B–E, mean ± SEM is plotted; * $p<0.05$ relative to tdT control transfectants (D) or to stromal cells treated with tdT control exosomes (E).

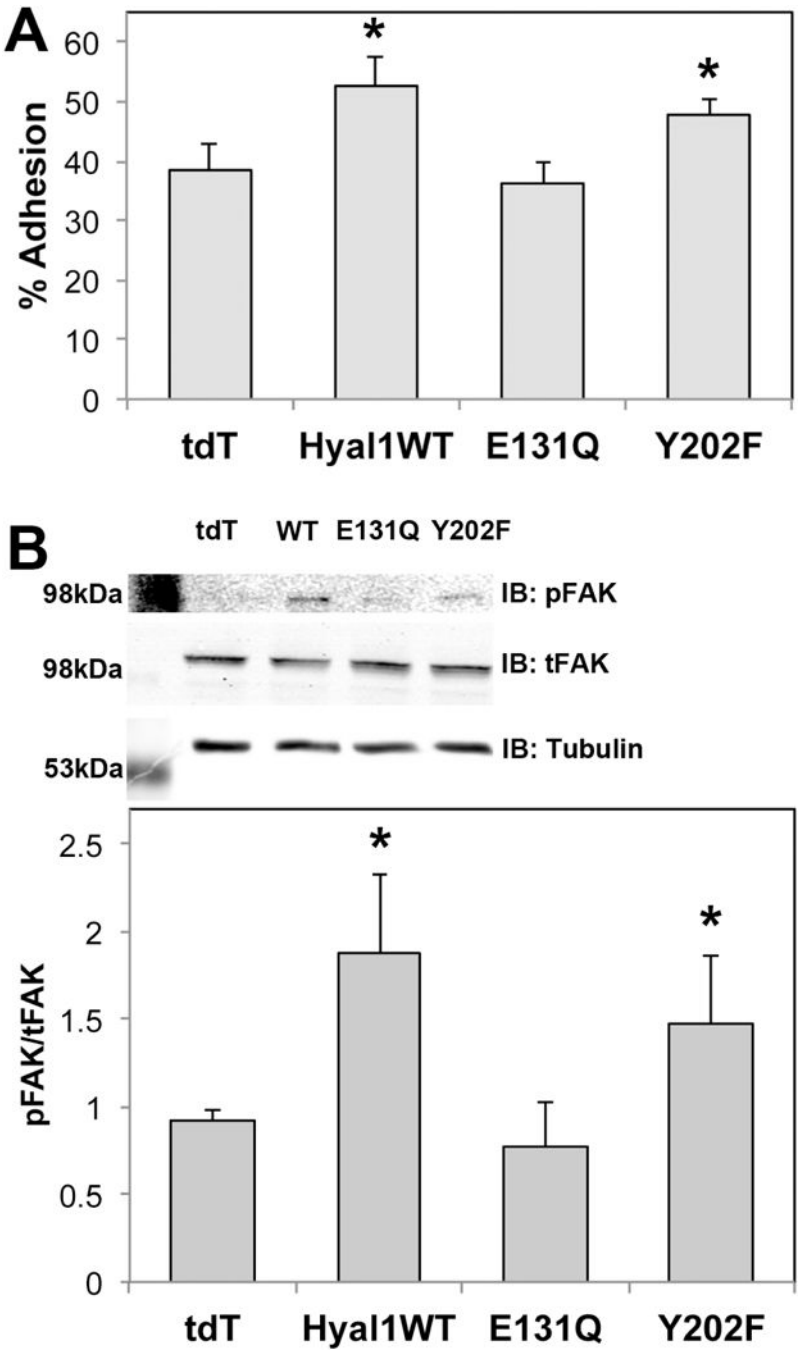

Figure 7.

Active Hyal1-containing exosomes accelerate stromal chemotaxis via increased ECM adhesion and activation of FAK phosphorylation. (A) Exosome-treated or untreated WPMY-1 cells were labeled with calcein-AM and seeded on type IV collagen coated microwell plates for 30 min at 37°C. Non-adherent cells were removed by washing and remaining adherent cells were quantified by fluorescence. (B) Exosome-treated or untreated WPMY-1 cells were seeded on type IV collagen coated plates. After two hours, adherent cells were lysed and equal amounts of protein were analyzed by western blot for

phosphorylated and total FAK, which was plotted as a ratio. In both panels, the mean ± SEM for triplicate wells is plotted; *$p<0.05$ relative to cells treated with tdT control exosomes.